JOURNAL OF GUIDANCE, CONTROL, AND DYNAMICS
Vol. 16, No. 1, January-February 1993

Designing Reduced-Order Linear Multivariable Controllers Using Experimentally Derived Plant Data

W. Garth Frazier* and R. Dennis Irwin†
Ohio University, Athens, Ohio 45701

An iterative numerical algorithm for simultaneously improving multiple performance and stability robustness criteria for multivariable feedback systems is developed. The unsatisfied design criteria are improved by updating the free parameters of an initial, stabilizing controller's state-space matrices. Analytical expressions for the gradients of the design criteria are employed to determine a parameter correction that improves all of the feasible, unsatisfied design criteria at each iteration. A controller design is performed using the algorithm with experimentally derived data from a large space structure test facility. Experimental results of the controller's performance at the facility are presented.

Nomenclature

I = identity matrix
$C^{n\times m}$ = set of complex-valued $n \times m$ matrices
R = set of real numbers
$R^{n\times m}$ = set of real-valued $n \times m$ matrices
$\mathrm{Re}[\cdot]$ = real part of a complex quantity
$\sigma_k[\cdot]$ = kth largest singular value of a matrix
$\partial f/\partial[\cdot]$ = matrix with (i,j) entry equal to $\partial f/\partial[\cdot]_{ij}$
$[\cdot]^H$ = complex-conjugate matrix transpose
$[\cdot]^T$ = matrix transpose
$\|\cdot\|$ = Euclidean norm of a vector

Introduction

IN recent years, renewed research interest in frequency-domain analysis techniques for multivariable linear time-invariant control systems has led to many new and important results.[1,2] Most control-law synthesis procedures proposed for achieving the constraints imposed by these results, such as linear-quadratic-Gaussian with loop transfer recovery (LQG/LTR) and more recently H_∞, require a mathematical model and considerable insight into the underlying mathematical theory to achieve a successful design. This insight is needed in selecting the proper weighting matrices or weighting functions to cast what is naturally a multiple-constraints satisfaction problem into an unconstrained optimization problem. Although designers possessing considerable experience with these techniques have a feel for the proper choice of weights, others may spend a significant amount of time attempting to find an acceptable solution.

As an alternative to these synthesis procedures, some numerical techniques have been proposed for achieving the constraints imposed by the results in Refs. 1 and 2. One technique that appears to be effective is that of Boyd et al.[3] and Boyd and Barratt.[4] Their approach is to cast the constraints for the design problem into a form such that the optimization is convex over the set of controllers that stabilize a given model of the system. Therefore, the solution is the global optimum and is obtained by standard mathematical programming techniques. Unfortunately, some constraints cannot be cast into a form that is closed-loop convex; important ones being open-loop controller stability, controller order, and controller structure (e.g., diagonal). A mathematical model of the plant is also required.

A method close in spirit to the technique presented here is that proposed by Newsom and Mukhopadhyay.[5] In their approach, the singular-value gradients of a return difference operator are used to iteratively change the parameters of a nominal controller in order to improve the stability robustness properties of a system. The parameter correction vector at each iteration is chosen to decrease a cumulative measure (sum of squares) of all constraint violations. The disadvantage of this correction vector is that, while the cumulative measure may improve, the worst violation is not guaranteed to improve. Recently, Mukhopadhyay[6] has extended the approach to incorporate other constraints, although a cumulative measure is still employed to monitor each constraint's improvement.

The algorithm presented here simultaneously includes performance constraints and stability robustness constraints. It also has the advantage that the worst constraint violations are improved at each iteration as long as the constraints are locally feasible in the parameter space.

Problem Formulation

The problem may be stated as follows: given 1) experimentally derived frequency-response data from a multivariable plant (continuous time or discrete time); 2) frequency-domain design constraints (and/or time-domain constraints that can be expressed in terms of frequency-dependent functions); and 3) an initial stabilizing controller of any order or structure, iteratively alter the free parameters of the controller to improve or, better yet, satisfy the design constraints. This is a multiple-constraint improvement problem and not an optimization problem. Unfortunately, this does not necessarily reduce the computational effort required to obtain an acceptable design.

A key point is the desire to use experimentally derived data taken from the multivariable plant. It is felt by the authors that in many cases this data is more reliable for design purposes than analytical models and models derived from system-identification procedures. This is especially so if the system is of "high" order as are many flexible aerospace structures. If a reliable model is available, an initial design could be done using analytical techniques and then an iterative technique applied to this initial design using experimental data for further design improvements.

The central issue in most parameter-search algorithms is the determination of an acceptable parameter correction vector at each iteration. This is often complicated by the existence of multiple constraints on various functions of the parameters. Achieving multiple constraints is precisely the problem faced

Received Sept. 23, 1991; revision received April 1, 1992; accepted for publication May 12, 1992.

*Ohio Aerospace Institute Fellow and Research Assistant, Department of Electrical and Computer Engineering, Stocker Center.

†Associate Professor, Department of Electrical and Computer Engineering, Stocker Center. Member AIAA.

in control system design when both performance and stability robustness requirements are specified. An effective approach to solving this type of problem was developed by Mitchell[7] and was applied to traditional gain and phase margin constraints. In this presentation, a similar approach is applied to frequency-dependent singular-value constraints relevant to multivariable feedback system performance and stability robustness.

Algorithm Description

Let

$$\Omega = \{\omega_i:\ i = 1,2,\ldots,N\} \tag{1}$$

be a set of frequencies at which the frequency-response data of the plant is available. Let

$$s = [s_1 \quad s_2 \quad \cdots \quad s_P]^T \tag{2}$$

denote a vector of parameters (elements of the state-space matrices of the controllers) on which the frequency-dependent functions

$$f_k(s) : \Omega_k \rightarrow \boldsymbol{R}, \qquad k = 1,2,\ldots,L \tag{3}$$

depend, where $\Omega_k \subset \Omega$ and Ω_k contain $N_k \leq N$ points. Define the design constraints by

$$f_k(\omega_j;s) > c_k(\omega_j) \forall \omega_j \in \Omega_k, \qquad k = 1,2,\ldots,L \tag{4}$$

where each $c_k : \Omega_k \rightarrow \boldsymbol{R}$ is defined according to the desired shape of f_k.

Now define the complete set of constraint violations by

$$S_v(s) = \cup_{k=1}^{L} \left\{ \cup_{j=1}^{N_k} \left[f_k(\omega_j;s) : f_k(\omega_j;s) \leq c_k(\omega_j) \right] \right\} \tag{5}$$

and denote the elements of $S_v(s)$ by $h_j(s)$, $j = 1,2,\ldots,N_v$, where N_v is the total number of violations. It follows (dropping the dependence on s for brevity) that the gradient of each h_j is given by

$$\boldsymbol{g}_j = \frac{\partial h_j}{\partial s} = \left[\frac{\partial h_j}{\partial s_1} \quad \frac{\partial h_j}{\partial s_2} \quad \cdots \quad \frac{\partial h_j}{\partial s_P} \right]^T, \quad j = 1,2,\ldots,N_v \tag{6}$$

A fundamental result from optimization theory is that to improve a single violation h_i, a parameter correction vector $\boldsymbol{d}$ must be chosen with the property $\boldsymbol{g}_i^T \boldsymbol{d} > 0$. Since, in general, there are many violations to be improved at any one iteration, $\boldsymbol{d}$ should be chosen to satisfy $\boldsymbol{g}_j^T \boldsymbol{d} > 0$, $j = 1,2,\ldots,N_v$. A sufficient condition for such a direction to exist is that the system

$$[\boldsymbol{g}_1 \quad \boldsymbol{g}_2 \quad \cdots \quad \boldsymbol{g}_{N_v}]^T \boldsymbol{d} = \boldsymbol{w} \tag{7}$$

be consistent, where

$$\boldsymbol{w} = [w_1 \quad w_2 \quad \cdots \quad w_j \quad \cdots \quad w_{N_v}]^T \tag{8}$$

and $w_j > 0$ for $j = 1,2,\ldots,N_v$. This is an $N_v \times P$ system of linear equations. In practice, Eq. (7) is almost always underdetermined because there are usually more free parameters than violations. Hence, there may be many solutions. To obtain the solution having minimum 2-norm, define

$$J = [\boldsymbol{g}_1 \quad \boldsymbol{g}_2 \quad \cdots \quad \boldsymbol{g}_{N_v}] \tag{9}$$

and suppose that J has rank r. Then J has the singular-value expansion[8]

$$J = \sum_{i=1}^{r} \sigma_i \boldsymbol{u}_i \boldsymbol{v}_i^T \tag{10}$$

where $\sigma_i > 0$, $i = 1,2,\ldots,r$, are the nonzero singular values of J and $\boldsymbol{u}_i$, $\boldsymbol{v}_i$, $i = 1,2,\ldots,r$, are the associated left and right singular vectors. If $\boldsymbol{w}$ is in the range of J^T, then

$$\boldsymbol{d} = \sum_{i=1}^{r} \sigma_i^{-1} (\boldsymbol{u}_i^T \boldsymbol{w}) \boldsymbol{v}_i \tag{11}$$

Although the preceding development indicates a general procedure for choosing an acceptable correction vector, it does not indicate how to choose the precise entries of $\boldsymbol{w}$ for good algorithm performance. Since it is desired to improve all of the violations simultaneously, it seems reasonable to choose $\boldsymbol{w}$ such that each of the violations is considered to be equally important. Following the development of Mitchell,[7] if the elements of $\boldsymbol{w}$ are chosen such that

$$w_j = \|\boldsymbol{g}_j\| \tag{12}$$

then from Eq. (7)

$$\boldsymbol{g}_j^T \boldsymbol{d} = \|\boldsymbol{g}_j\|, \qquad j = 1,2,\ldots,N_v \tag{13}$$

Using the fact that

$$\boldsymbol{g}_j^T \boldsymbol{d} = \|\boldsymbol{g}_j\| \, \|\boldsymbol{d}\| \cos \Theta_j = \|\boldsymbol{g}_j\| \tag{14}$$

where Θ_j is the angle between $\boldsymbol{g}_j$ and $\boldsymbol{d}$, it is clear that

$$\cos \Theta_j = \|\boldsymbol{d}\|^{-1}, \qquad j = 1,2,\ldots,N_v \tag{15}$$

Therefore, this choice results in a correction vector that forms an equal angle between itself and each $\boldsymbol{g}_j$.

Because of the nonlinearity of the parameter space, it is necessary to determine a satisfactory step length for the correction vector at each iteration. In most iterative algorithms, the determination of the step length at each iteration is treated as an optimization problem. Unfortunately, this optimization can require many constraint function evaluations and would be computationally prohibitive in this algorithm.

Therefore, the choice of an appropriate step-length parameter at each iteration is based on several other criteria: 1) maintaining closed-loop stability, 2) maintaining open-loop controller stability properties, and 3) improvement of the violated constraints. To maintain closed-loop stability using discrete frequency data (as opposed to a mathematical model), the multivariable Nyquist criterion[9] is employed. Although it is not a reliable indicator of relative stability margins, it has proven effective in this algorithm for maintaining closed-loop stability. Controller stability is achieved by simply monitoring the controller's poles. Although controller stability is not an absolute requirement, it is desirable in most applications, e.g., when loop failure is possible. As for the third criterion, the violated constraints are simply checked for improvements at each iteration. If they have improved, the parameter vector is updated and the step length is increased by a user-defined factor for use at the next iteration. If not, the step length is reduced and the constraints are checked again. This process is repeated until improvements are registered or until the minimum step length allowed is reached. If the minimum step length is reached, then either a violated constraint has reached a local minimum or two gradients are in local opposition. In the case of a local minimum, the design can either be accepted or the constraint relaxed. The action to be taken if two gradients are opposed is now discussed.

In the case of two gradients in local opposition, the matrix J will be nearly rank deficient and the correction vector $\boldsymbol{d}$, although defined, will almost be orthogonal to all of the gradient vectors. Hence, improving the constraints with an acceptable step length is highly unlikely. If one of the opposing gradients is not associated with the worst violation for that particular constraint, the problem can be circumvented by dropping that gradient from J at the current iteration. If, however, both gradients are associated with the worst viola-

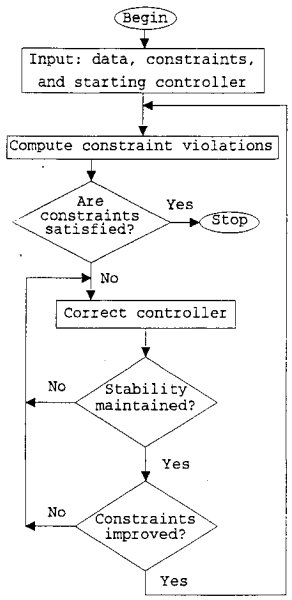

Fig. 1 Flowchart of the design algorithm.

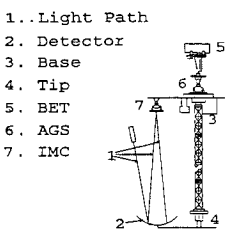

Fig. 2 Schematic of the ACES structure.

tions of different constraints, then the constraints are not locally feasible and this technique will fail to improve the constraints. Hence, the algorithm is not guaranteed to satisfy all of the design constraints, but it will improve the violated constraints until no further local improvement is possible. It is also important to note that even if the constraints are satisfied, they are only satisfied at the frequencies for which the design was performed. A flowchart of the complete algorithm is given in Fig. 1.

Design Example

A schematic of the NASA Marshall Space Flight Center (MSFC) Active Control Technique Evaluation for Spacecraft (ACES) structure is shown in Fig. 2. The ACES structure is suitable for the study of line-of-sight (LOS) and vibration-suppression control issues as pertaining to flexible aerospace structures. The primary element of the ACES structure, a spare Voyager magnetometer boom, is a lightly damped beam measuring approximately 45 ft in length and weighing about 5 lb.

The goal of the control system design is to maintain the reflected laser beam in the center of the antenna (location of the detector) in the presence of disturbances at the base excitation table (BET). This is to be accomplished by use of the following actuators: image motion compensation (IMC) gimbals (2 axes), advanced gimbal system (AGS) (3 axes), linear momentum exchange devices (LMEDs) (two 2-axes devices); and the sensors: base rate gyros (3 axes), tip accelerometers (3 axes), tip rate gyros (3 axes), LMED positions and accelerations (2 axes each), and the optical position detector (2 axes). As explained subsequently, our design only employed a subset of these sensors and actuators. The digital controller is to be implemented on the HP9000 computer located at the facility using the fixed sampling rate of 50 Hz and a fixed, one-sample-period computational delay. The results of other controller designs for the ACES structure have been reported in the literature.[10]

The experimental open-loop frequency response from the y-axis IMC gimbal to the x-axis LOS error is shown in Fig. 3. The effect of the computational delay is quite apparent from analysis of the phase characteristic. The frequency responses of the other axes of the IMC-to-LOS are similar, although the cross-axis terms have less gain. The open-loop frequency response from the y-axis AGS gimbal to the y-axis base gyro is shown in Fig. 4. This response reveals the numerous lightly damped modes of the structure. The frequency responses of other elements of the AGS-to-base gyros transfer matrix are similar. It is noted that the cross-axis elements have considerable gains at some modal frequencies.

The basic design philosophy was to dampen the pendulum modes and the bending modes of the beam by using feedback from the base gyros to the AGS while using the IMC gimbals with feedback from the detector to maintain the laser beam at the center of the detector. Because of sufficient decoupling, each two-input, two-output subsystem (AGS and IMC) was designed separately. One concern was the impact of disturbances that reach the IMC gimbals through the connecting arm that is attached to the base (as opposed to disturbances impacting the detector). Because of the inherently high optical gain from the IMC to the detector, these disturbances can have a significant impact on the LOS error. To compensate for the effects of these disturbances, it is not only necessary to maintain high loop gain over the frequency band of interest, but to also maintain high gain in the IMC controller as well. Analysis of Fig. 3 reveals that achieving high controller gain while also maintaining acceptable stability margins is difficult because of the combination of the high optical gain and the additional phase lag introduced by the computational delay. Fortunately, the impact of these disturbances can also be reduced by increasing the damping of the modes of the beam using the AGS, thereby reducing the motion of the base and the arm supporting the IMC gimbals.

The first step of the design procedure was the determination of a set of precise closed-loop constraints such as those given in the first column of Table 1. These particular constraints (inherently multivariable in nature) are consistent with the philosophy of the design. In particular, the fifth constraint is included to suppress the effect of a lightly damped pendulum

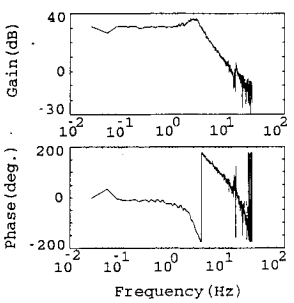

Fig. 3 Experimental frequency response from y-axis IMC gimbal to x-axis LOS error.

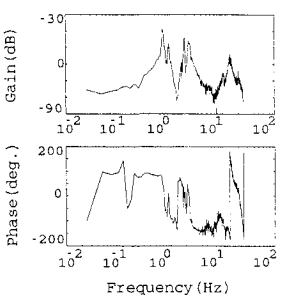

Fig. 4 Experimental frequency response from y-axis AGS gimbal to y-axis base gyro.

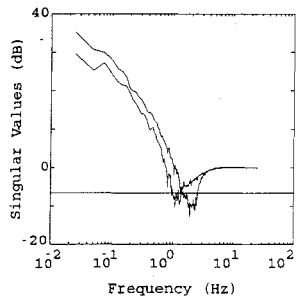

Fig. 5 Initial singular-value frequency response of $(I+GK)_{IMC}$.

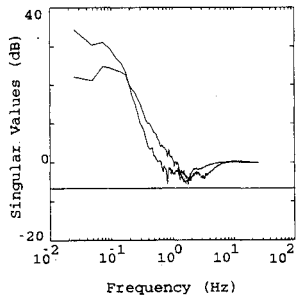

Fig. 6 Final singular-value frequency response of $(I+GK)_{IMC}$.

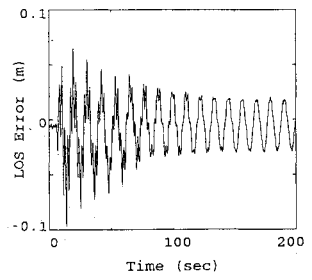

Fig. 7 Open-loop x-axis LOS error.

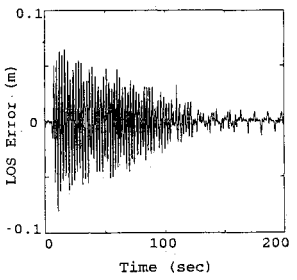

Fig. 8 The x-axis LOS error only using LOS error feedback.

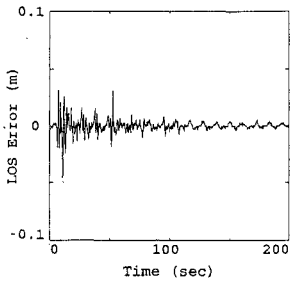

Fig. 9 The x-axis LOS error using LOS error feedback and base gyro feedback.

Table 1 Summary of multivariable design constraints

Constraint	Initial	Final
$\sigma_{\min}[I+GK(z)]_{IMC}>0.5, f\in(0,25)$	0.2289	0.5090
$\sigma_{\min}[I+KG(z)]_{IMC}>0.5, f\in(0,25)$	0.2276	0.5056
$\sigma_{\min}[I+(GK(z))^{-1}]_{IMC}>0.6, f\in(0,25)$	0.2827	0.6072
$\sigma_{\min}[I+(KG(z))^{-1}]_{IMC}>0.6, f\in(0,25)$	0.2805	0.6112
$\sigma_{\min}[I+GK(z)]_{IMC}>18, f=0.15$	10.002	14.100
$\sigma_{\min}[I+GK(z)]_{AGS}>0.6, f\in(0,25)$	0.3649	0.5996
$\sigma_{\min}[I+KG(z)]_{AGS}>0.6, f\in(0,25)$	0.3585	0.5988
$\sigma_{\min}[I+(GK(z))^{-1}]_{AGS}>0.7, f\in(0,25)$	0.3600	0.6719
$\sigma_{\min}[I+(KG(z))^{-1}]_{AGS}>0.7, f\in(0,25)$	0.3589	0.6712

Note: IMC represents IMC subsystem. AGS represents AGS subsystem. G represents plant. K represents controller. $z=e^{j2\pi fT}$, $T=0.02$ s.

mode. The gradients for these and other constraint functions for a somewhat generalized feedback system are provided in the Appendix. Next, initial stabilizing controllers were designed for the IMC-to-LOS loops and for the AGS-to-base gyro loops using one-loop-at-a-time graphical techniques with experimental data. The effects of cross-axis coupling were ignored except for stability purposes. As a result, the constraints were far from being satisfied as can be observed by comparing the first and second columns in Table 1. The controller for each subsystem was tenth order. It should be noted that recently developed high-fidelity models are 60th order for the AGS-to-base gyro loops alone. Design techniques such as LQG and H^{∞} would yield controllers of at least this order (not including weighting).

The multivariable design (i.e., taking cross-axis coupling within each subsystem into account) for each subsystem was then performed using only experimental data and the presented algorithm. The algorithm was started with the initial tenth-order controllers just described, with no restrictions other than stability placed on the structure of the controllers. Implementation was on an Intel 80386 based personal computer. To illustrate typical results from the algorithm, Figs. 5 and 6 show the experimental singular-value frequency responses of the return difference matrix $[I+GK]_{IMC}$ of the initial and final controllers, respectively. The final values of all of the constraint functions are given in the third column of Table 1. The constraints for the AGS subsystem were not satisfied because the algorithm reached a point such that these constraint functions were in the condition of "local opposition" described previously.

The resulting controller was implemented at the ACES facility. The open-loop x-axis LOS error due to an x-axis BET disturbance intended to simulate the effect of spacecraft crew motion is shown in Fig. 7. The dominant behavior in the response is the lightly damped 0.15-Hz pendulum mode. After closing only the IMC-to-LOS loops, the steady-state error and the impact of the pendulum mode were reduced as shown in Fig. 8. However, the first bending mode was still present. As shown in Fig. 9, closing the IMC-to-LOS and the AGS-to-base gyro loops further reduced the impact of the pendulum mode and almost eliminated the first bending mode. Similar results were obtained for the y-axis LOS error.

The decrease in the LOS error with the AGS-to-base gyro loops closed can be explained by the fact that significant damping was added to the pendulum mode and the first bending mode. The same disturbance was applied with the y axis of the BET and results quite similar to those presented here were obtained for the various measured outputs.

Conclusions

An iterative numerical technique for the design of linear multivariable controllers has been presented. The technique has been shown to have the advantages that 1) multiple closed-loop design constraints can be simultaneously considered without the need for weighting schemes and the attendant increase in controller order; 2) the design engineer can have complete control over controller order and structure; 3) the design can

be performed with or without the use of a parametric plant model; and 4) locally feasible, violated constraints can be improved at each iteration.

The application of the technique to a controller design for a large aerospace structure test facility has been presented. Experimental results were also presented and appear to be very promising. The resulting controller order was low (20th) as compared to designs that would result from using techniques such as linear-quadratic-Gaussian with loop transfer recovery.

Although the presented design example only involves constraints on matrix singular-value frequency responses, there is no reason that the technique could not be applied to other constraints such as the shapes of individual elements of frequency-response matrices and rms measures when such constraints are of interest.

Appendix: Generalized Gradients

Because of the importance of the gradients in the aforementioned algorithm, the analytical expressions for the gradients of an arbitrary real-valued function of a controller's state-space matrices (for which the partial derivatives exist) is needed. Let the response of a discrete-time controller at a single frequency ω_i be given by

$$K(e^{j\omega_i T}) = C\Phi_i B + D \tag{A1}$$

where $\Phi_i = (e^{j\omega_i T}I - A)^{-1}$. Let f be a real-valued function of the controller K. Then it is not difficult to show that

$$\frac{\partial f}{\partial D} = \mathrm{Re}\left[\left(\frac{\partial f}{\partial K}\right)^H\right]^T \tag{A2}$$

$$\frac{\partial f}{\partial C} = \mathrm{Re}\left[\Phi_i B\left(\frac{\partial f}{\partial K}\right)^H\right]^T \tag{A3}$$

$$\frac{\partial f}{\partial B} = \mathrm{Re}\left[\left(\frac{\partial f}{\partial K}\right)^H C\Phi_i\right]^T \tag{A4}$$

$$\frac{\partial f}{\partial A} = \mathrm{Re}\left[\Phi_i B\left(\frac{\partial f}{\partial K}\right)^H C\Phi_i\right]^T \tag{A5}$$

Since singular values play a significant role in modern linear multivariable system analysis, the case when f is a singular value of some frequency-dependent system transfer matrix is of particular importance. Let $T \in \boldsymbol{C}^{n\times n}$. Then T admits a singular-value decomposition (SVD) $T = U\Sigma V^H$, where $U \in \boldsymbol{C}^{n\times n}$ and $V \in \boldsymbol{C}^{n\times n}$ are unitary matrices and $\Sigma \in R^{n\times n}$ is a diagonal matrix with nonnegative entries. Let p be a real-valued parameter such that T is a function of p, i.e., $T = T(p)$. Assuming nonrepeated singular values, the partial derivatives of the singular values of T with respect to p are given by

$$\frac{\partial \sigma_k(T)}{\partial p} = \mathrm{Re}\left(\boldsymbol{u}_k^H \frac{\partial T}{\partial p} \boldsymbol{v}_k\right), \qquad k = 1,2,\ldots,n \tag{A6}$$

where $\boldsymbol{u}_k$ and $\boldsymbol{v}_k$ are the columns of U and V, respectively.[11] Using Eqs. (A2–A6), the partials of the singular values of various closed-loop transfer matrices with respect to the controller state-space matrices can be calculated to form the gradient expressions.

To develop the expressions for a generalized linear time-invariant feedback system, consider the block diagram given in Fig. A1. Each block represents a transfer matrix (the dependence on frequency is excluded for brevity) and is defined as follows:

G_1: plant
G_2: output disturbance effect
G_3: input disturbance effect
H_1: sensors
H_2: sensor noise effect
K_1: forward path controller defined as $K_1 = C_1\Phi_1 B_1 + D_1$
K_2: feedback path controller defined as $K_2 = C_2\Phi_2 B_2 + D_2$

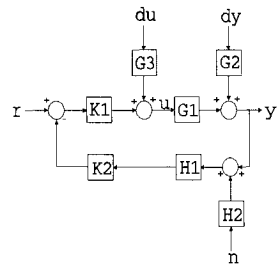

Fig. A1 Generalized feedback system.

where $\Phi_i = (e^{j\omega T}I - A_i)^{-1}$, $i = 1,2$, for discrete-time systems. The signals are defined as follows:

$\boldsymbol{r}$: reference
$\boldsymbol{u}$: control
$\boldsymbol{y}$: quantity to be controlled
$\boldsymbol{n}$: sensor noise
$\boldsymbol{d}_u$: input disturbance
$\boldsymbol{d}_y$: output disturbance

Define the loop responses

$$L_y = G_1K_1K_2H_1 \tag{A7}$$

$$L_u = K_1K_2H_1G_1 \tag{A8}$$

and the usual sensitivity functions

$$S_u = (I + L_u)^{-1} \tag{A9}$$

$$S_y = (I + L_y)^{-1} \tag{A10}$$

Likewise, the complementary sensitivity functions are defined by

$$T_u = L_u(I + L_u)^{-1} \tag{A11}$$

$$T_y = L_y(I + L_y)^{-1} \tag{A12}$$

Hence, the following transfer relations hold

$$\boldsymbol{y} = G_{yr}\boldsymbol{r} + G_{yd_y}\boldsymbol{d}_y + G_{yd_u}\boldsymbol{d}_u + G_{yn}\boldsymbol{n} \tag{A13}$$

and

$$\boldsymbol{u} = G_{ur}\boldsymbol{r} + G_{ud_u}\boldsymbol{d}_u + G_{ud_y}\boldsymbol{d}_y + G_{un}\boldsymbol{n} \tag{A14}$$

where

$$G_{yr} = S_yG_1K_1, \quad G_{yd_y} = S_yG_2, \quad G_{yd_u} = S_yG_1G_3$$

$$G_{yn} = -T_yH_2, \quad G_{ur} = S_uK_1, \quad G_{ud_y} = -S_uK_1K_2H_1G_2$$

$$G_{ud_u} = S_uG_3, \quad G_{un} = -S_uK_1K_2H_1H_2$$

Singular-value gradients for these transfer relations are given below. The vectors $\boldsymbol{v}_k$ and $\boldsymbol{u}_k$ in the following expressions are the singular vectors associated with the kth singular value of the SVD of the corresponding transfer relation. Only the partials with respect to the controller matrices K_1 and K_2 are given since the gradients with respect to the state-space matrices can be obtained simply by substituting these results in Eqs. (A2–A5).

Return difference for input node (S_u^{-1}):

$$\frac{\partial \sigma_k(S_u^{-1})}{\partial K_1} = (K_2H_1\boldsymbol{v}_k\boldsymbol{u}_k^HG_1)^H \tag{A15}$$

$$\frac{\partial \sigma_k(S_u^{-1})}{\partial K_2} = (H_1G_1\boldsymbol{v}_k\boldsymbol{u}_k^HK_1)^H \tag{A16}$$

Inverse complementary sensitivity for output node $T_y^{-1} = I + (L_y)^{-1}$:

$$\frac{\partial \sigma_k(T_y^{-1})}{\partial K_1} = -(K_2 H_1 L_y v_k u_k^H L_y G_1)^H \quad \text{(A17)}$$

$$\frac{\partial \sigma_k(T_y^{-1})}{\partial K_2} = -(H_1 L_y v_k u_k^H L_y G_1 K_1)^H \quad \text{(A18)}$$

Inverse complementary sensitivity for input node $T_u^{-1} = I + (L_u)^{-1}$:

$$\frac{\partial \sigma_k(T_u^{-1})}{\partial K_1} = -(K_2 H_1 G_1 L_u v_k u_k^H L_u)^H \quad \text{(A19)}$$

$$\frac{\partial \sigma_k(T_u^{-1})}{\partial K_2} = -(H_1 G_1 L_u v_k u_k^H L_u K_1)^H \quad \text{(A20)}$$

Transfer from reference to output (G_{yr}):

$$\frac{\partial \sigma_k(G_{yr})}{\partial K_1} = \left[(I - K_2 H_1 S_y G_1 K_1) v_k u_k^H S_y G_1\right]^H \quad \text{(A21)}$$

$$\frac{\partial \sigma_k(G_{yr})}{\partial K_2} = -[H_1 S_y G_1 K_1 v_k u_k^H S_y G_1 K_1]^H \quad \text{(A22)}$$

Transfer from output disturbance to ouput (G_{yd_y}):

$$\frac{\partial \sigma_k(G_{yd_y})}{\partial K_1} = -(K_2 H_1 S_y G_2 v_k u_k^H S_y G_1)^H \quad \text{(A23)}$$

$$\frac{\partial \sigma_k(G_{yd_y})}{\partial K_2} = -(H_1 S_y G_1 v_k u_k^H S_y G_1 K_1)^H \quad \text{(A24)}$$

Transfer from input disturbance to output (G_{yd_u}):

$$\frac{\partial \sigma_k(G_{yd_u})}{\partial K_1} = -(K_2 H_1 S_y G_1 G_3 v_k u_k^H S_y G_1)^H \quad \text{(A25)}$$

$$\frac{\partial \sigma_k(G_{yd_u})}{\partial K_2} = -(H_1 S_y G_1 G_3 v_k u_k^H S_y G_1 K_1)^H \quad \text{(A26)}$$

Transfer from sensor noise to output (G_{yn}):

$$\frac{\partial \sigma_k(G_{yn})}{\partial K_1} = -[K_2 H_1 S_y H_2 v_k u_k^H S_y G_1]^H \quad \text{(A27)}$$

$$\frac{\partial \sigma_k(G_{yn})}{\partial K_2} = -[H_1 S_y H_2 v_k u_k^H S_y G_1 K_1]^H \quad \text{(A28)}$$

Transfer from reference to input (G_{ur}):

$$\frac{\partial \sigma_k(G_{ur})}{\partial K_1} = \left[(I - K_2 H_1 G_1 S_u K_1) v_k u_k^H S_u\right]^H \quad \text{(A29)}$$

$$\frac{\partial \sigma_k(G_{ur})}{\partial K_2} = -(H_1 G_1 S_u K_1 v_k u_k^H S_u K_1)^H \quad \text{(A30)}$$

Transfer from output disturbance to input (G_{ud_y}):

$$\frac{\partial \sigma_k(G_{ud_y})}{\partial K_1} = \left[(K_2 H_1 G_1 S_u K_1 - I) K_2 H_1 G_2 v_k u_k^H S_u\right]^H \quad \text{(A31)}$$

$$\frac{\partial \sigma_k(G_{ud_y})}{\partial K_2} = \left[(H_1 G_1 S_u K_1 K_2 - I) H_1 G_2 v_k u_k^H S_u K_1\right]^H \quad \text{(A32)}$$

Transfer from input disturbance to input (G_{ud_u}):

$$\frac{\partial \sigma_k(G_{ud_u})}{\partial K_1} = -(K_2 H_1 G_1 S_u G_3 v_k u_k^H S_u)^H \quad \text{(A33)}$$

$$\frac{\partial \sigma_k(G_{ud_u})}{\partial K_2} = -(H_1 G_1 S_u G_3 v_k u_k^H S_u K_1)^H \quad \text{(A34)}$$

Transfer from sensor noise to input (G_{un}):

$$\frac{\partial \sigma_k(G_{un})}{\partial K_1} = \left[(K_2 H_1 G_1 S_u K_1 - I) K_2 H_1 H_2 v_k u_k^H S_u\right]^H \quad \text{(A35)}$$

$$\frac{\partial \sigma_k(G_{un})}{\partial K_2} = \left[(H_1 G_1 S_u K_1 K_2 - I) H_1 H_2 v_k u_k^H S_u K_1\right]^H \quad \text{(A36)}$$

Acknowledgments

The authors would like to thank NASA Marshall Space Flight Center for support under NAG8-123(21) and the Ohio Aerospace Institute for its support. Thanks is also due Henry Waites, Alan Patterson, and Jerrel Mitchell.

References

[1]Doyle, J. C., and Stein, G., "Multivariable Feedback Design: Concepts for a Clasical/Modern Synthesis," *IEEE Transactions on Automatic Control,* Vol. AC-26, No. 1, Feb. 1981, pp. 4–16.

[2]Safonov, M. G., Laub, A. J., and Hartman, G. L., "Feedback Properties of Multivariable Systems: The Role and Use of the Return Difference Matrix," *IEEE Transactions on Automatic Control,* Vol. AC-26, No. 1, Feb. 1981, pp. 47–65.

[3]Boyd, S. P., Balakrishnan, V., Barratt, C., Khraishi, N., Li, X., Meyer, D., and Norman, S., "A New CAD Method and Associated Architectures for Linear Controllers," *IEEE Transactions on Automatic Control,* Vol. 33, No. 3, March 1988, pp. 268–283.

[4]Boyd, S. P., and Barratt, C. H., *Linear Controller Design: Limits of Performance,* Prentice-Hall, Englewood Cliffs, NJ, 1991, Chap. 6.

[5]Newsom, J. R., and Mukhopadhyay, V., "A Multiloop Robust Controller Design Study Using Singular Value Gradients," *Journal of Guidance, Control, and Dynamics,* Vol. 8, No. 4, 1985, pp. 514–519.

[6]Mukhopadhyay, V., "Digital Robust Control Law Synthesis Using Constrainted Optimization," *Journal of Guidance, Control, and Dynamics,* Vol. 12, No. 2, 1989, pp. 175–181.

[7]Mitchell, J. R., "An Innovative Approach to Compensator Design," Ph.D. Dissertation, State College, MS, May 1972.

[8]Golub, G. H., and Van Loan, C. F., *Matrix Computations,* 2nd ed., Johns Hopkins Univ. Press, Baltimore, MD, 1989, p. 72.

[9]Postlethwaite, I., and MacFarlane, A. G. J., *A Complex Variable Approach to the Analysis of Linear Multivariable Feedback Systems,* Springer-Verlag, New York, 1979.

[10]Collins, E. G., Jr., Phillips, D. J., and Hyland, D. C., "Robust Decentralized Control Laws for the ACES Structure," *IEEE Control Systems Magazine,* Vol. 11, No. 3, April 1991, pp. 62–70.

[11]Junkins, J. L., and Kim, Y., "First- and Second-Order Sensitivity of the Singular-Value Decomposition," *Journal of the Astronautical Sciences,* Vol. 38, No. 1, 1990, pp. 69–86.